

Parametric plasmonics and second harmonic generation in particle chains

Ben Z. Steinberg*

School of Electrical Engineering, Tel Aviv University, Ramat-Aviv, Tel-Aviv 69978 Israel

[*steinber@eng.tau.ac.il](mailto:steinber@eng.tau.ac.il)

Abstract: Parametric optics and second harmonic generation in pure plasmonic particle chains are studied. By a proper design of the plasmonic particle geometry, the modes supported by the chain can achieve phase-matching conditions. Then the magnetic-field dependence of the plasmon electric susceptibility can provide the nonlinearity and the coupling mechanism leading to parametric processes, sum frequency and second harmonic generation. Hence, chains of plasmonic particles can support parametric optics and higher harmonic generation by using its own modes only. Since the second order nonlinearity involves both electric and magnetic fields, the SHG reported here is supported also by centrosymmetric particle chains.

© 2011 Optical Society of America

OCIS codes: (250.5403) Plasmonics; (190.4410) Nonlinear optics and parametric processes; (190.2620) Harmonic generation and mixing.

References and links

1. M. Quinten, A. Leitner, J. R. Krenn, and F. R. Aussenegg, "Electromagnetic energy transport via linear chains of silver nanoparticles," *Opt. Lett.* **23**(17), 1331-1333 (1998).
2. S. A. Tretyakov and A. J. Viitanen, "Line of periodically arranged passive dipole scatterers," *Electrical Engineering* **82**, 353-361 (2000).
3. M. L. Brongersma, J. W. Hartman, H. A. Atwater, "Electromagnetic energy transfer and switching in nanoparticle chain arrays below the diffraction limit," *Phys. Rev. B* **62**(24), R16356 (2000).
4. Andrea Alu and Nader Engheta, "Theory of linear chains of metamaterial/plasmonic particles as subdiffraction optical nanotransmission lines," *Phys. Rev. B* **74**, 205436 (2006).
5. D. V. Orden, Y. Fainman, and V. Lomakin, "Optical waves on nanoparticle chains coupled with surfaces," *Opt. Lett.* **34**(4), 422-424 (2009).
6. D. V. Orden, Y. Fainman, and V. Lomakin, "Twisted chains of resonant particles: optical polarization control, waveguidance, and radiation," *Opt. Lett.* **35**(15), 2579-2581 (2010).
7. Y. Hadad and Ben Z. Steinberg, "Magnetized spiral chains of plasmonic ellipsoids for one-way optical waveguides," *Phys. Rev. Lett.* **105**, 233904 (2010).
8. Zi-jian Wu, Xi-kui Hu, Zi-yan Yu, Wei Hu, Fei Xu, and Yan-qing Lu, "Nonlinear plasmonic frequency conversion through quasiphase matching," *Phys. Rev. B* **82**, 155107 (2010).
9. A. R. Davoyan, I. V. Shadrivov, and Y. S. Kivshar, "Quadratic phase matching in nonlinear plasmonic nanoscale waveguides," *Opt. Express* **17**(22), 20063-20068 (2009).
10. G. Bachelier, I. R. Antoine, E. Benichou, C. Jonin, and P. F. Brevet, "Multipolar second-harmonic generation in noble metal nanoparticles," *J. Opt. Soc. Am. B* **25**(6) 955-960 (2008).
11. Y. Zeng, W. Hoyer, J. Liu, S. W. Koch, and J. Moloney, "Classical theory for second-harmonic generation from metallic nanoparticles," *Phys. Rev. B* **79**, 235109 (2009).
12. H. Husu, J. Makitalo, J. Laukkanen, M. Kuittinen, and M. Kauranen, "Particle plasmon resonance in L-shaped gold nano-particles," *Opt. Express* **18**(16), 16601-16606 (2010).
13. J. Nappa, G. Revillod, I. R. Antoine, E. Benichou, C. Jonin, and P. F. Brevet, "Electric dipole origin of the second harmonic generation of small metallic particles," *Phys. Rev. B* **71**, 165407 (2005).
14. J. Shan, J. I. Dadap, I. Stiopkin, G. A. Reider, and T. F. Heinz, "Experimental study of optical second-harmonic scattering from spherical nanoparticles," *Phys. Rev. A* **73**, 023819 (2006).

15. B. K. Canfield, H. Hsu, J. Laukkanen, B. Bai, M. Kuittinen, J. Turunen, and M. Kauranen, "Local field asymmetry drives second-harmonic generation in noncentrosymmetric nanodimers," *Nano Letters* **7**(5), 1251-1255 (2007).
16. S. Kujala, B. K. Canfield, and M. Kauranen, "Multipole interference of second harmonic optical radiation from gold nanoparticles," *Phys. Rev. Lett.* **98**, 167403 (2007).
17. T. Utikel, T. Zentgraf, T. Paul, C. Rockstuhl, F. Lederer, M. Lippitz, and H. Giessen, "Towards the origin of the nonlinear response in hybrid plasmonic systems," *Phys. Rev. Lett.* **106**, 133901 (2011).
18. J. D. Jackson, *Classical Electrodynamics*, 3rd ed. (Wiley 1999).
19. S. A. Maier, P. G. Kik, and H. A. Atwater, "Optical pulse propagation in metal nanoparticle chain waveguides," *Phys. Rev. B* **67**, 205402 (2003).
20. A. H. Sihvola *Electromagnetic Mixing Formulas and Applications*, Electromagnetic Waves Series (IEE 1999).
21. Leonard Lewin, *Polylogarithms and Associated Functions* (Elsevier 1981).
22. M. Abramowitz and I. A. Stegun *Handbook of Mathematical Functions* (Dover 1972).

1. Introduction

Linear chains of identical and equally-closely-spaced plasmonic particles have been studied in a number of publications [1–4]. It has been shown that they allow the propagation of optical modes with relatively low attenuation and with no radiation to the free space. This property is obtained if the inter-particle distance is smaller than the free space wavelength λ , and then the total width of the modes can be much smaller than λ . Hence the name "Sub-Diffraction Chains" (SDC). SDCs are potential candidates for dense integration of optical systems, and were proposed as guiding structures, junctions, and couplers [1–5], as chiral waveguides [6], and also as one-way waveguides [7].

In this work we study parametric optics and second harmonic generation (SHG) in plasmonic particle SDC's. Plasmonic structures can support highly localized electromagnetic modes, and therefore have the potential to enhance nonlinear processes. Essentially two different physical schemes can be invoked. In the first, the plasmonic structure is used mainly for field concentration and enhancement while the non-linearity is provided by another dielectric material (such as LiNbO₃) [8, 9]. In the second scheme, the inherent non-linear response of metallic nano-particles and structures is exploited. SHG processes associated with a single particle, particle arrays or dispersed particles were studied theoretically and experimentally in a number of publications [10–16]. (The non-trivial issue of distinguishing between the two processes in combined plasmonic-dielectric structures is discussed, e.g. in [17].) In these works special attention is given to the particle symmetry; non-centrosymmetry is essential for locally excited dipole-induced SHG if the nonlinear dipole response depends solely on the electric field. This well known restriction is due to the fact that under space inversion ($\mathbf{r} \mapsto -\mathbf{r}$) one has $\mathbf{p} \mapsto -\mathbf{p}$ and $\mathbf{E} \mapsto -\mathbf{E}$, so we must have $\chi_{ee}^{(2)} = 0$. It was shown that centrosymmetric particles can support SHG either by locally excited quadrupoles, or by nonlocal excitations of dipoles (see e.g. [13, 14] and references therein). However, the centrosymmetry exclusion can be alleviated; non-centrosymmetry is essential for locally excited dipole-induced SHG *only if* the nonlinear dipole response depends solely on the electric field. Under space inversion $\mathbf{H} \mapsto \mathbf{H}$, so SHG *can be supported by centrosymmetric particles if the nonlinear dipole response depends on \mathbf{E} and \mathbf{H}* (e.g. it involves terms as $\mathbf{H} \times \mathbf{E}$ due to Lorentz force). As we shall see, the underlying physics associated with SHG in our chains is in line with these general observations.

To efficiently utilize the potential of parametric gain and SHG, one needs a constructive interference of the generated radiation, commonly manifested by phase-matching conditions. Hence, our study is based on two essential steps. First, the dispersion relations of the SDC modes are examined. By a proper design of the chains particles, phase matching between the supported modes can be achieved. The key is to use ellipsoidal particles rather than the conventional spherical ones-see Fig. 1(a). The second step is of fundamental importance; we use the non-linearity resulting from the plasmonic susceptibility dependence on magnetic fields [18],

to establish coupling between the magnetic fields of one of the modes, and the electric *polarization* of another mode. The physical process underlying the non-linearity is schematized in Fig. 1(b). Two important points should be emphasized. First, it is essentially a Lorentz force term, so SHG is supported even with centrosymmetric particles such as the ellipsoids shown in the figure. Second, the nonlinearity at any given particle in the chain, is excited due to magnetic fields created by its neighbors that can be viewed as retarded-field non-local contributions (in analogy with bulk-theories, it comes from other particles in the bulk). Again consistently with previous publications non-local dipole contributions can support SHG in centrosymmetric particles. Hence, our ellipsoids-based SDC can amplify or generate optical signals constructively *using its own modes only*.

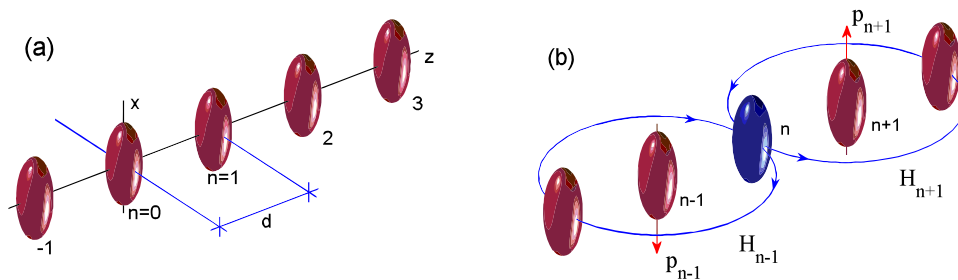


Fig. 1. A subdiffraction chain of ellipsoidal particles ($d \ll \lambda$). Resonances, phase-matching conditions, and gain can be achieved by designing d and the ellipsoids semi-axis a_x, a_y, a_z . (a) Chain Geometry for prolate ellipsoid particles. (b) Source of non-linearity. The chain supports a modal dipole response of the form $\mathbf{p}_m = \hat{x}p_0 e^{im\beta}$. We examine the specific case of $\beta \approx \pi/2$; for any n , there is a phase difference of π between the dipole responses of the two nearest neighbors of the n -th particle. As a result their (\hat{y} -directed) magnetic fields add constructively at the n -th site, creating a modulation of the n -th particle (in blue) *electric* susceptibility component relevant for a \hat{z} -directed dipole. Hence a parametric coupling between the \hat{x} and the \hat{z} polarized dipole excitations is created, both can be supported by the chain dispersion. Generally, at the n -th site, the magnetic fields of the $n \pm \ell$ neighbors add constructively (destructively) for odd (even) ℓ . The strongest contributions are from $\ell = 1$. This general picture holds also if β deviates from $\pi/2$. In fact, the maximal value of \mathbf{H} is obtained for $\beta \approx 0.4\pi$.

In our analysis we use the Discrete Dipole Approximation (DDA) and polarizability theory, in conjunction with the Nearest Neighbor Approximation (NNA). The former two are standard tools used in many works on SDCs [3–6]. They hold when the particle diameter D is much smaller than the wavelength so it can be considered as an infinitesimal dipole, and the inter-particle distance d is large compare to D . Studies show excellent agreement with exact solutions even when d and D are of the same order [19]. To simplify the analysis and to obtain transparent analytical results, we employ the nearest neighbor approximation (NNA). Here, one assumes that the field exciting the n -th particle is mainly due to its two nearest neighbors, namely due to particles $n \pm 1$. Since the electric near field of an infinitesimal dipole behaves essentially as $(kr)^{-3}$, this approximation holds very well for SDCs with inter-particle distance $d \ll \lambda$. Indeed it was shown that chain dispersions resulting from the NNA are in excellent agreement with those of the full theory if $d/\lambda \leq 0.1$ [4], but good agreement is obtained even with larger ratios such as $d/\lambda \approx 0.25$ [3]. As shown in these two early studies, there is only one exception: the dispersion of the transverse modes near the light line is not predicted well by the NNA. We keep away from this domain and concentrate in regions where it holds well. Since dispersions

play here the pivotal role for the phase-matching, the NNA discussed in [3, 4] provides the phase-matching conditions in a sufficient accuracy.

2. Formulation

If a small particle with electric polarizability tensor or matrix $\underline{\alpha}$ is subject to an exciting electric field whose local value in the *absence of the particle* is \mathbf{E}^L , its response is described by the electric dipole $\mathbf{p} = \underline{\alpha}\mathbf{E}^L$. The matrix (or tensor) polarizability of a general ellipsoid made of an anisotropic dielectric material with electric matrix-susceptibility $\underline{\chi}$ can be found in [20] for the static case. In the dynamic case it needs to be augmented to incorporate radiation loss, but consistently with the NNA [3,4] this correction is neglected here. If the ellipsoid principal axes are aligned with the x, y, z axes, its polarizability $\underline{\alpha}$ is

$$\underline{\alpha} = \epsilon_0 V \left(\mathbf{I}_3 + \underline{\chi}\underline{\mathbf{L}} \right)^{-1} \underline{\chi} \quad (1)$$

Here \mathbf{I}_3 is the 3 by 3 identity matrix, $V = 4\pi a_x a_y a_z / 3$ is the ellipsoid volume and a_x, a_y, a_z are its semiaxes. $\underline{\mathbf{L}} = \text{diag}(N_x, N_y, N_z)$ is the depolarization matrix whose entries are obtained by elliptic integrals and satisfy $\sum_u N_u = 1$ [20]. We give some canonical examples. A sphere has $N_u = 1/3 \forall u$. A *prolate* ellipsoid ($a_x > a_y = a_z = a$), has $N_y = N_z = (1 - N_x)/2$, $N_x = (1 - e^2) \{ \ln[(1+e)/(1-e)] - 2e \} / (2e^3)$, where $e = (1 - a^2/a_x^2)^{1/2}$. Hence a “football” with $a_x = 2a$ has $N_x \approx 0.1736, N_z \approx 0.4132$. An *oblate* ellipsoid ($a_x = a_y = a > a_z$) has $N_x = N_y = (1 - N_z)/2$, $N_z = (1 + e^2)(e - \arctan e)/e^3$, where $e = (a^2/a_z^2 - 1)^{1/2}$. Hence a “m&m” with $a_z = a/3$ has $N_z \approx 0.6354, N_x \approx 0.1823$.

$\underline{\chi}$ of magnetized plasmons is obtained by applying Lorentz force. Up to first order in the magnetization field \mathbf{H} , it is given by (see appendix)

$$\underline{\chi} = \chi_{ee} [\mathbf{I}_3 + i\underline{\mathbf{B}}_H], \quad \chi_{ee} = -\frac{\omega_p^2}{\omega(\omega + i/\tau)} \quad (2)$$

where the scalar χ_{ee} is the non-magnetized plasma susceptibility [18]. Up to a constant factor, the matrix operator $\underline{\mathbf{B}}_H$ is equivalent to a vector multiplication by the magnetic field \mathbf{H} from left,

$$\underline{\mathbf{B}}_H = \frac{e\mu_0}{\omega m_e} \begin{pmatrix} 0 & -H_z & H_y \\ H_z & 0 & -H_x \\ -H_y & H_x & 0 \end{pmatrix} \equiv \frac{e\mu_0}{\omega m_e} \mathbf{H} \times \quad (3)$$

and \times is the vector product. The time constant τ represents material loss. In practical situations this loss is orders of magnitude larger than the particle radiation loss [3]. We note that the equation above is valid as long as χ_{ee} is valid for non-magnetized metals. No assumption is made about the rate of change of \mathbf{B} ; Lorentz force holds for any time-scale. The expression above can be obtained also as a first order approximation (in \mathbf{B}) of the magnetized plasma susceptibility given in [18].

Let \mathbf{p}_n be the n -th particle dipole moment. Under the DDA and the NNA, it is excited only by its two nearest neighbors. Hence it is governed by the difference equation [3] (assume $kd \ll 1$ and use the expression for the near field of an infinitesimal dipole [18])

$$\mathbf{p}_n = \frac{1}{4\pi\epsilon_0 d^3} \underline{\alpha} [3\hat{z}(\hat{z} \cdot \mathbf{S}_n) - \mathbf{S}_n] \quad (4)$$

where \mathbf{S}_n is the nearest-neighbors sum,

$$\mathbf{S}_n \equiv \mathbf{p}_{n+1} + \mathbf{p}_{n-1}. \quad (5)$$

Equations (1)-(5) constitute a starting point for various parametric processes in particle chains under the discrete dipole and nearest neighbor approximations.

2.1. Dispersion and phase matching

We first examine phase-matching conditions when loss may be neglected ($1/\tau \rightarrow 0$), and when the non-linearity due to \mathbf{B}_H can be neglected. By substituting the solution

$$\mathbf{p}_n = \mathbf{p}_0 e^{i\beta n} \quad (6)$$

into Eq. (4) and using the linear part of Eq. (2), we obtain the *three independent* dispersion relations, governing the transverse (x, y) and longitudinal (z) independent polarizations

$$(\omega/\omega_p)^2 = N_u + \sigma_u \cos(\beta), \quad u = x, y, z \quad (7)$$

here $(\sigma_x, \sigma_y, \sigma_z) = (\sigma, \sigma, -2\sigma)$, with $\sigma = V/(2\pi d^3)$, where $\sigma < N_u \forall u$. We look for solutions that satisfy the SHG condition or the sum frequency generation (SFG) condition,

$$\text{SHG: } (\omega_3, \beta_3) = (2\omega_1, 2\beta_1) \quad (8)$$

$$\text{SFG: } (\omega_3, \beta_3) = (\omega_1 + \omega_2, \beta_1 + \beta_2). \quad (9)$$

For spherical particles $N_u = 1/3 \forall u$, so Eq. (7) reduces to the known dispersions [3, 4], all centered around $\omega_p/\sqrt{3}$; they cannot support Eqs. (8)–(9). However, by using ellipsoidal particles one can design the central frequencies $\omega_p \sqrt{N_u}$ such that the dispersions in Eq. (7) can satisfy the conditions in Eq. (8) or Eq. (9). We start with SHG. Of particular interest is a solution that supports for wave#1 a \hat{x} polarized mode at its central frequency, and for wave#3 a \hat{z} polarized mode [see Fig. 1(b)]. By imposing Eq. (8) on the corresponding dispersions in Eq. (7), we obtain

$$N_z - 4N_x = 2\sigma [\cos(2\beta_1) + 2\cos(\beta_1)] \quad (10)$$

It is all about chain-particle geometry. Using the expressions for the prolates and oblates N_u 's [see discussion after Eq. (1)] and σ , the ellipsoid parameter a_x/a_z and particles separation parameter a_x/d satisfying the above equation were computed for geometrically feasible configurations ($d > 2a_z$). The results are shown in Fig. 2(a). For general ellipsoids, more solutions may be available.

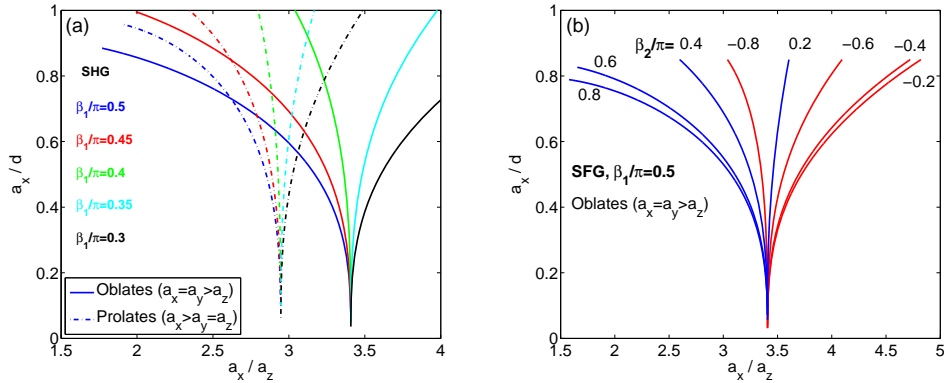


Fig. 2. Geometrical parameters of prolate or oblate ellipsoid SDC, supporting (a) SHG of Eq. (8) for various values of β_1 , and (b) SFG of Eq. (9) for various values of β_2 .

For the SFG in Eq. (9), we still look for \hat{x} -polarized wave as mode#1, but now with \hat{y}, \hat{z} -polarized modes#2,3, respectively. With the dispersions in Eq. (7) and with $\beta_1 = \pi/2$, Eq. (9) becomes

$$\sigma \cos(\beta_2) + 2(N_x N_y + N_x \sigma \cos \beta_2)^{1/2} = 2N_z - 1 \pm 2\sigma \sin \beta_2. \quad (11)$$

where we used $\sum N_u = 1$. Solutions for oblates are shown in Fig. 2(b). Again, other solutions are available for general ellipsoids and/or other polarizations and/or other values of β_1 .

2.2. Nonlinear chain dynamics

We turn now to explore the SDC dynamics under self-magnetization. It is the magnetic field of the SDC modes that establishes the non-linearity via Eqs. (2)–(3), the actual mode coupling, and eventually gain and SHG. However, it is inconvenient to express the non-linearity directly with the magnetic field of the SDC mode. Instead, we express the chain magnetization in terms of one of the SDC modes dipole moments, that will later play the role of the pump wave. Note that \mathbf{H} of the mode under the NNA has not been studied before. The NNA validity for \mathbf{H} is not as transparent as for \mathbf{E} , since for electric dipole the near H-field goes up as r^{-2} while the near E-field as r^{-3} . Hence, below we first make an exact evaluation of the mode magnetic field (i.e. considering contributions from all the chain particles), and then compare it to the magnetic field obtained under the NNA (i.e. contributions from the two closest neighbors only). We show the range of parameters for which the two results do not differ much (the specific examples shown later, however, use the exact field).

The magnetic field at $(0, 0, nd)$ due to a single electric dipole \mathbf{p}_m at $(0, 0, md)$, is given by [18]

$$\mathbf{H}_{nm} = \hat{z} \times \mathbf{p}_m \operatorname{sgn}(m-n) ck^2 g(d_{mn}) [1 + i/(kd_{mn})] \quad (12)$$

where $d_{mn} = d|m-n|$, $g(x) = e^{ikx}/(4\pi x)$, and $\operatorname{sgn}(u) = u/|u|$. The magnetic field at the location of the n -th dipole is given by summing \mathbf{H}_{nm} in Eq. (12) over m , $m \neq n$, and using Eq. (6) for \mathbf{p}_m . The self magnetic field of the n -th particle, \mathbf{H}_{nn} , is excluded as it averages to zero over the particle volume. The result is

$$\mathbf{H}_n = \sum_{m, m \neq n} \mathbf{H}_{nm} = \hat{z} \times \mathbf{p}_n \frac{ck^3}{4\pi} F(kd, \beta) \quad (13)$$

where

$$F(kd, \beta) = \frac{1}{kd} \left[Li_1(e^+) - Li_1(e^-) + \frac{i}{kd} Li_2(e^+) - \frac{i}{kd} Li_2(e^-) \right], \quad e^\pm \equiv e^{ikd \pm i\beta} \quad (14)$$

and where Li_s is the s -th order Polylogarithm function [21] defined as

$$Li_s(z) = \sum_{n=1}^{\infty} \frac{z^n}{n^s} \quad \Rightarrow \quad Li_0(z) = \frac{z}{1-z}, \quad Li_1(z) = -\ln(1-z). \quad (15)$$

$Li_s(e^{i\theta})$ are expressable in terms of the Clausen's integral and series, for which efficient summation formulas are available (see Sec. 27.8 in [22]). The exact \mathbf{H}_n in absolute value and in units of $\hat{z} \times \mathbf{p}_n ck^3/(4\pi)$ is shown in Fig. 3(a). For $kd \ll 1$ the magnetization strength is maximal for $\beta \approx 0.4\pi$. For larger values of kd another maximum emerges along the light line $\beta = kd$. Note however that the chain supports propagating modes in the form of Eq. (6) only for $\beta > kd$ [4], hence the magnetization field shown in the figure is supported by the chain modes only above this line.

To get a feeling of the field structure, consider the SDC mode near its central frequency $\mathbf{p}_m = \mathbf{p}_0 e^{im\beta}$, $\beta \approx \pi/2$. The magnetic field is still given by the sum in Eq. (13), with Eq. (12). Since $\beta \approx \pi/2$ and due to the sgn term in Eq. (12), contributions from odd neighbor-pairs $m = n \pm (2\ell + 1)$, $\ell = 0, 1, \dots$ add up *constructively* at n ; most important, this includes the nearest neighbor-pair $n \pm 1$ whose contribution is the strongest possible. Likewise, contributions from even neighbor-pairs $m = n \pm 2\ell$, $\ell = 1, 2, \dots$ add up *destructively* and cancel out. The

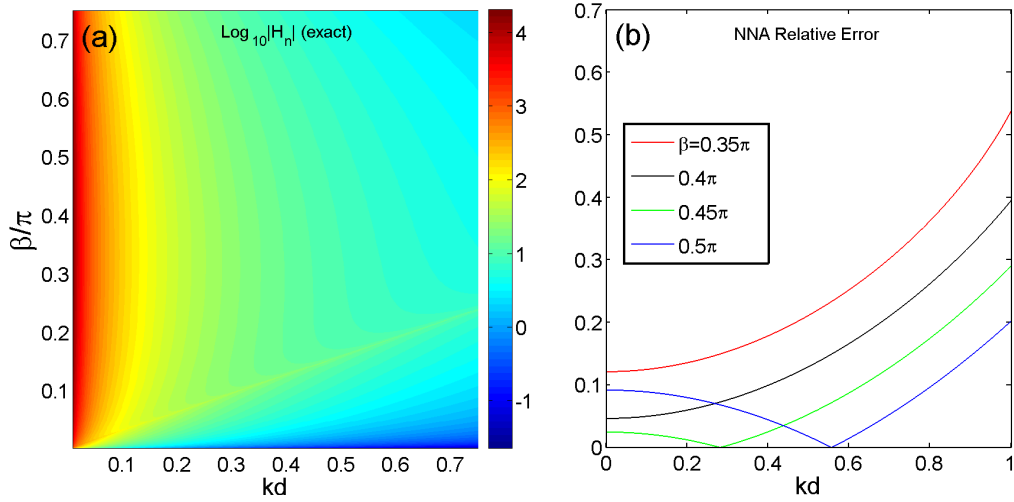


Fig. 3. The n -th particle magnetization due to the chain's own electric-dipole mode. (a) The exact \mathbf{H}_n of Eq. (15) shown in the $kd, \beta/\pi$ plane. The field is in units of $\hat{z} \times \mathbf{p}_n c k^3 / (4\pi)$ on logarithmic scale. (b) The NNA error for values of β , near $\pi/2$.

physical picture is schematized in Fig. 1(b). Consistent with the NNA (valid for $kd \ll 1$), we keep only the contributions from the pair $m = n \pm 1$ and neglect the rest; the next non-zero term is an order of magnitude weaker. We end up with an expression similar to that of Eq. (13), where $F(kd, \beta)$ is approximated by

$$F(kd, \beta) \approx -\frac{2}{(kd)^2} \sin \beta. \quad (16)$$

The exact F and its NNA are compared in Fig. 3(b). For $\beta/\pi \approx 0.4 : 0.5$ the error of the NNA is less than 10% for kd up to 0.4.

With the mode self-magnetization of Eqs. (13)–(16) we may establish the non-linear dynamics. Using it in Eqs. (1)–(3), and substituting the result in Eq. (4), we obtain the non-linear formulation (multiply on left by $\mathbf{I}_3 + \chi \mathbf{L}$ and rearrange),

$$[(\omega/\omega_p)^2 + i\omega/(\omega_p^2 \tau)] \mathbf{p}_n = \mathbf{L} \mathbf{p}_n - (\sigma/2) [3\hat{z}(\hat{z} \cdot \mathbf{S}_n) - \mathbf{S}_n] + \Psi \quad (17)$$

where τ^{-1} is the loss term, σ is defined after Eq. (7), the vector Ψ represents the non-linear dynamics [use vector identities e.g. $(\mathbf{a} \times \mathbf{b}) \times \mathbf{c} = \mathbf{b}(\mathbf{a} \cdot \mathbf{c}) - \mathbf{a}(\mathbf{b} \cdot \mathbf{c})$ etc],

$$\Psi = iA [\mathbf{p}_n(\hat{z} \cdot \mathbf{L} \mathbf{p}_n) - \hat{z}(\mathbf{p}_n \cdot \mathbf{L} \mathbf{p}_n)] - iA (\sigma/2) [2\mathbf{p}_n(\hat{z} \cdot \mathbf{S}_n) + \hat{z}(\mathbf{S}_n \cdot \mathbf{p}_n) - 3\hat{z}(\hat{z} \cdot \mathbf{p}_n)(\hat{z} \cdot \mathbf{S}_n)] \quad (18)$$

and

$$A = A(kd, \beta) = \frac{k^2 e \mu_0}{4\pi m_e} F(kd, \beta). \quad (19)$$

Under the DDA and NNA, Eqs. (17)–(18) constitute a self-consistent formulation for general second order parametric optics in plasmonic SDC's.

3. Second harmonic generation

We show the existence of SHG process that satisfies Eq. (8). The analysis is based on the conventional approach: write the various waves in Eqs. (17)–(18) with their time dependence,

add their complex conjugate, and look for terms at frequencies and polarizations of interest. Let wave#1 be a \hat{x} polarized SDC mode with ω_1, β_1 satisfying the corresponding linear ideal (lossless) dispersion relation Eq. (7). Likewise, let wave#3 be a \hat{z} polarized SDC mode, with ω_3, β_3 satisfying the corresponding dispersion relation in Eq. (7) and the SHG phase matching condition in Eq. (8). This is possible by virtue of the results shown in Fig. 2. We express these modes in a slight generalization of Eq. (6),

$$\mathbf{p}_n^{(1)} = \hat{x} \tilde{p}_n^{(1)} e^{i\beta_1 n}, \quad \mathbf{p}_n^{(3)} = \hat{z} \tilde{p}_n^{(3)} e^{i\beta_3 n} \quad (20)$$

where $\tilde{p}_n^{(i)}, i = 1, 3$ depend on n to allow for possible loss, and for gain or depletion due to mutual interactions. We turn to obtain the dynamic equation for the ω_3 oscillations from the formulation in Eqs. (17)–(18). For compactness, we also define

$$\tilde{S}_n^{(1,3)} = \tilde{p}_{n+1}^{(1,3)} e^{i\beta_{1,3}} + \tilde{p}_{n-1}^{(1,3)} e^{-i\beta_{1,3}} \quad (21)$$

To get both sides of Eq. (17) to oscillate at $\omega_3 = 2\omega_1$ the linear terms should incorporate only wave#3, and Ψ should incorporate only wave#1. The former is \hat{z} -polarized. The surviving \hat{z} directed terms in Ψ that contribute to ω_3 oscillations are the second one ($\mathbf{p}_n^{(1)} \cdot \mathbf{L} \mathbf{p}_n^{(1)}$) and ($\mathbf{S}_n^{(1)} \cdot \mathbf{p}_n^{(1)}$). Hence Eq. (17) gets the form

$$\left[(\omega_3/\omega_p)^2 + i\omega_3/(\omega_p^2 \tau) \right] \tilde{p}_n^{(3)} = N_z \tilde{p}_n^{(3)} - \sigma \tilde{S}_n^{(3)} - i(A_1/4) \tilde{p}_n^{(1)} \left[\sigma \tilde{S}_n^{(1)} + 2N_x \tilde{p}_n^{(1)} \right]. \quad (22)$$

In the above, $A_1 = A(k_1 d, \beta_1)$ where $A(kd, \beta)$ is defined in equations Eq. (16) (this is because the magnetization field, presented by A , is due to wave#1). Likewise, to get both sides of Eq. (17) to oscillate at ω_1 the linear terms should incorporate only wave#1, and Ψ should incorporate only multiplications between waves#1 and #3. The only surviving terms are $[\mathbf{p}_n^{(1)}]^* (\hat{z} \cdot \mathbf{L} \mathbf{p}_n^{(3)})$ and $[\mathbf{p}_n^{(1)}]^* (\hat{z} \cdot \mathbf{S}_n^{(3)})$. Hence Eq. (17) becomes

$$\left[(\omega_1/\omega_p)^2 + i\omega_1/(\omega_p^2 \tau) \right] \tilde{p}_n^{(1)} = N_x \tilde{p}_n^{(1)} + (\sigma/2) \tilde{S}_n^{(1)} - i(A_1/2) [\tilde{p}_n^{(1)}]^* \left[\sigma \tilde{S}_n^{(3)} - N_z \tilde{p}_n^{(3)} \right]. \quad (23)$$

Equations (22)-(23) describe the interaction between the two waves (and consequently SHG) in a self-consistent manner. To facilitate transparent analytical solution, we assume that wave#1 is of high intensity and is not depleted due to energy transfer to wave#3. Below, two cases of the SHG under the non-depleted pump are considered.

3.1. Non depleted pump with $\beta_1 = \pi/2$ in lossless chain

We examine the ideal (lossless) chain case, with non-depleted pump wave at its central frequency $(\omega_1, \beta_1) = (N_x^{1/2}, \pi/2)$. We further assume that wave#3 is zero at the chain origin. Hence, we look for a solution satisfying

$$\tilde{p}_n^{(1)} = \tilde{p}_0^{(1)} \forall n, \quad \tilde{p}_0^{(3)} = 0. \quad (24)$$

With the above parameters, $\tilde{S}_n^{(1)} = 0$, so Eq. (22) for the second harmonic wave $\tilde{p}_n^{(3)}$ reduces to

$$(\omega_3/\omega_p)^2 \tilde{p}_n^{(3)} = N_z \tilde{p}_n^{(3)} - \sigma \tilde{S}_n^{(3)} - iN_x (A_1/2) \left[\tilde{p}_0^{(1)} \right]^2. \quad (25)$$

By direct substitution, it is easily verified that an *exact* solution to Eq. (25), that satisfies the initial condition in Eq. (24), is given by [use $(\omega_3/\omega_p)^2 = N_z + 2\sigma, \beta_3 = 2\beta_1 = \pi$, as implied by Eqs. (7)–(8)] and their solution in Fig. 2]

$$\tilde{p}_n^{(3)} = iN_x (A_1/4\sigma) \left[\tilde{p}_0^{(1)} \right]^2 n^2. \quad (26)$$

It is seen that the SDC's second-harmonic wave grows as n^2 - a quadratic growth typical to SHG.

3.2. Chain with loss

We solve now Eqs. (22)–(23) under lossy conditions and for pump wave not necessarily at $(\omega_1, \beta_1) = (\sqrt{N_x}, \pi/2)$, but still with the exact phase matching conditions in Eq. (8). Note that the mode magnetization (which carries the gain) is maximized at $\beta_1 \approx 0.4\pi$ - see Fig. 3. We “generalize” the non-depleted pump assumption to hold for a lossy medium: we assume that the pump attenuation is mainly due to loss mechanism, and the attenuation due to energy transfer to wave# 3 can be neglected. Hence, we have for the pump:

$$\tilde{p}_n^{(1)} = \tilde{p}_0^{(1)} e^{-\gamma n} \quad (27)$$

The attenuation factor γ can be computed by generalizing the dispersion relation to hold for complex β [4]. Typical values for Ag particles, for example, are $\gamma \approx 0.1 : 0.15$ [1, 3]. Since the chain is lossy, and the pump itself decreases exponentially, we have the following initial/final conditions for wave# 3:

$$\tilde{p}_0^{(3)} = 0, \quad \lim_{n \rightarrow \infty} \tilde{p}_n^{(3)} = 0. \quad (28)$$

Substituting $\tilde{p}_n^{(1)}$ of Eq. (27) into Eq. (22) and rearranging, we obtain for $\tilde{p}_n^{(3)}$

$$B \tilde{p}_n^{(3)} + e^{i\beta_3} \tilde{p}_{n+1}^{(3)} + e^{-i\beta_3} \tilde{p}_{n-1}^{(3)} = [\tilde{p}_0^{(1)}]^2 D e^{-2\gamma n} \quad (29)$$

where

$$B = -2 \cos \beta_3 + \frac{i\omega_3}{\omega_p^2 \tau \sigma}, \quad D = -\frac{iA_1}{2\sigma} [N_x + \sigma \cosh(\gamma - i\beta_1)]. \quad (30)$$

The solution to the difference Eq. (29) consists of two terms. The first is the particular solution $\tilde{p}_n^{(3),p}$ that due to the forcing on the rhs it should be proportional to $e^{-2\gamma n}$. A straightforward substitution of $a e^{-2\gamma n}$ into the equation shows that the particular solution is given by

$$\tilde{p}_n^{(3),p} = [\tilde{p}_0^{(1)}]^2 a_p e^{-2\gamma n}, \quad a_p = \frac{D}{B + 2 \cosh(2\gamma - i\beta_3)}. \quad (31)$$

The second term is the homogeneous solution that satisfies the homogeneous counterpart (no forcing) of Eq. (29). It has the form $\tilde{p}_n^{(3),h} = a r^n$, where r is obtained by substituting this solution into the homogeneous equation and looking for the roots of the characteristic polynomial

$$r^2 + B e^{-i\beta_3} r + e^{-2i\beta_3} = 0 \Rightarrow r_{1,2} = \frac{e^{-i\beta_3}}{2} \left(B \pm \sqrt{B^2 - 4} \right). \quad (32)$$

Note that $r_1 r_2 = e^{-2i\beta_3}$. A careful examination shows that one of the roots, say r_1 , satisfies $|r_1| < 1$. Thus, the solution that satisfies Eq. (29) and the boundary conditions in Eq. (28) is

$$\tilde{P}_n^{(3)} = [\tilde{p}_0^{(1)}]^2 a_p (e^{-2\gamma n} - r_1^n). \quad (33)$$

It is interesting to point out that the solution for lossless chain with $\beta_1 = \pi/2$ studied in Sec.3.1 cannot be obtained by a mere substitution of $\beta_1 = \pi/2, 1/\tau = 0$ in Eq. (33). For $\beta_1 = \pi/2, 1/\tau = 0$ the characteristic polynomial has a higher order root multiplicity, in which case the solution must be written in terms of powers of n .

It may be convenient to cast the last results in terms of the chain electric fields, rather than the dipole moments. Let $\mathbf{E}_n^{(1,L)} = \hat{x} \tilde{E}_n^{(1)} e^{i\beta_1 n}$ be the n -th particle local field associated with chain mode#1, and $\mathbf{E}_n^{(3,L)} = \hat{z} \tilde{E}_n^{(3)} e^{i\beta_3 n}$ be that for mode#3. They are related to their respective dipole moments via the polarizability $\underline{\alpha}$. Hence

$$\tilde{E}_n^{(3)} = \frac{(\underline{\alpha}_1 \hat{x})^2}{\underline{\alpha}_3 \hat{z}} [\tilde{E}_0^{(1)}]^2 a_p (e^{-2\gamma n} - r_1^n). \quad (34)$$

where $\alpha_{1,3} = \alpha(\omega_{1,3})$.

Finally, it is interesting to examine the *local* ratio between the pump wave and the second harmonic. This ratio is given by

$$\frac{\tilde{E}_n^{(3)}}{\tilde{E}_n^{(1)}} = \frac{(\alpha_1 \hat{x})^2}{\alpha_3 \hat{z}} \tilde{E}_0^{(1)} a_p (e^{-2\gamma n} - r_1^n) e^{\gamma n}. \quad (35)$$

Hence, there is a critical value for r_1 : if $|r_1| > e^{-\gamma}$ this ratio increases unboundedly as the waves propagate along the chain, signifying an efficient energy transfer from the pump to the second harmonic. Clearly, for very large n the non-depleted assumption in lossy chain, defined at this subsection onset, ceases to be valid.

The efficiency of plasmonic SDC based SHG, is somewhat subtle to define. Since any plasmonic structure is considerably lossy, it is clear that the pump itself decreases exponentially due to loss, independently of the rate of energy transfer to SH. Then, its ability to "pump" also decreases exponentially. Any plasmonic mode undergoes this typical decay due to loss. Hence, Eq. (35) suggests a better-suited figure for the efficiency in the presence of loss. It actually provides two measures. (1) The *local* ratio between the signal and the pump as stated before; (2) the value of the signal when the typical loss decay is "cleaned out" (due to the multiplication by $e^{\gamma n}$). As will be shown in the example below, the result is exponentially increasing, with typical numerical values shown in Fig. 4.

A design example is in order. Consider a SDC of Ag prolates, in which a \hat{x} polarized pump wave propagates with $\beta_1 = 0.4\pi$. To achieve SHG phase-matching, we choose $a_x/d = 0.5$, and we use Fig. 2(a) and get $a_x/a_z \approx 2.93$, $\Rightarrow N_x \approx 0.112$. Solving for the corresponding complex dispersion relation with Ag loss factor $1/(\tau\omega_p) = 2 \cdot 10^{-3}$ we get $\omega_1 = 0.3323\omega_p$ and $\gamma = 0.143$. For Ag, $\omega_p \approx 8.6 \cdot 10^{15}$ rad/sec, hence $\omega_1 = 2.86 \cdot 10^{15}$ so $\lambda_1 = 660\text{nm}$. The prolates are spaced by $d = 80\text{nm}$, hence $a_x \approx 40\text{nm}$, $a_z \approx 14\text{nm}$, and $\sigma = V/(2\pi d^3) = 0.0097$. We used these parameters to compute the SHG in Eqs. (34)–(35), with the exact magnetization field in Eqs. (13)–(15). The results are shown in Fig.4 for $\tilde{E}_0^{(1)} = 1\text{V/m}$. For this example $|r_1| = 0.8915 > e^{-\gamma} = 0.8668$, thus the local ratio between the second harmonic and the pump increases along the array.

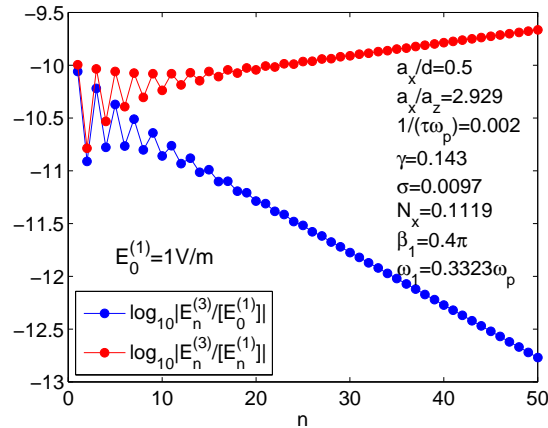


Fig. 4. SHG example in a lossy plasmonic chain, for pump of 1V/m at the chain input.

4. Summary

A formulation governing parametric processes and second harmonic generation in sub-diffraction chains of plasmonic particles has been developed. Phase matching conditions between the different modes supported by the chain can be achieved by a proper design of the particle geometry. Specific particle designs discussed here in detail are prolate and oblate ellipsoids, but in principle other geometries may be used too. Then, the plasma electric susceptibility dependence on magnetic fields is used to establish the nonlinearity and coupling between the magnetic field of a transversely-polarized e-dipole chain mode, and a longitudinally-polarized e-dipole mode. The formulation is general and applies to any second-order parametric process, but special emphasis is placed on SHG. Since the coupling process is essentially a Lorentz-force mechanism, the resulting SHG can be supported by centrosymmetric particle chains. Specific examples in the non-depleted pump approximation and in lossy chains are considered.

A. Derivation of Eq. (2)

We derive the plasmonic susceptibility under the weak \mathbf{H} -field assumption. Since the force exerted by \mathbf{H} on the free charge is *velocity dependent*, and since \mathbf{H} is assumed to be weak, we present the charge displacement as $\mathbf{r} = \mathbf{r}_1 + \mathbf{r}_2$ where the former is due to the electric field \mathbf{E} and the latter is a correction due to \mathbf{H} and due to the movement exerted by \mathbf{E} . Hence, up to first order in \mathbf{H} , the Lorentz force induced electron displacement is governed by

$$m_e \ddot{\mathbf{r}}_2 = -e\mu_0 \dot{\mathbf{r}}_1 \times \mathbf{H} \quad (36)$$

We assume that \mathbf{E} and \mathbf{H} oscillate at frequencies ω_1 and ω_2 , respectively (these are not Phasors; time dependence is included). Hence \mathbf{r}_1 and \mathbf{r}_2 possess $e^{-i\omega_1 t}$ and $e^{-i(\omega_1+\omega_2)t}$ time dependencies, respectively. Equation (36) reads now

$$\mathbf{r}_2 = \frac{-i\omega_1 e}{\omega_3^2 m_e} \mathbf{r}_1 \times \mathbf{B} \quad (37)$$

where $\omega_3 = \omega_1 + \omega_2$. Since charge displacement is proportional to dipole volume density, we have

$$\mathbf{P}_2 = \frac{-i\omega_1 e}{\omega_3^2 m_e} \mathbf{P}_1 \times \mathbf{B} \quad \Rightarrow \quad \mathbf{P}_2 = \frac{-i\omega_1 e}{\omega_3^2 m_e} \chi_{ee}(\omega_1) \mathbf{E} \times \mathbf{B} \quad (38)$$

where $\mathbf{P}_{1,2}$ are the dipole volume densities associated with the displacements $\mathbf{r}_{1,2}$ respectively. The scalar $\chi_{ee}(\omega) = -\omega_p^2 / [\omega(\omega + i/\tau)]$ is the electric susceptibility in the absence of magnetization, derived e.g. in [18]. The last result can be re-written as

$$\mathbf{P}_2 = \frac{i\omega_1 e}{\omega_3^2 m_e} \chi_{ee} \mathbf{B} \times \mathbf{E}^L \quad \Rightarrow \quad \mathbf{P} = \mathbf{P}_1 + \mathbf{P}_2 = \chi_{ee}(\omega_1) \left(\mathbf{I}_3 + \frac{ie}{\omega_1 m_e^*} \mathbf{B} \times \right) \mathbf{E} \quad (39)$$

where $m_e^* = [1 + \omega_2/\omega_1]^2 m_e$ is an effective measure of the electron mass. Note that in parametric processes and SHG the typical relations between ω_1 and ω_2 imply that $m_e^*/m_e = \mathcal{O}(1)$. Equation (39) is in fact the result written in Eqs. (2)–(3).

Acknowledgment

This research was supported by the Israel Science Foundation (grant 1503/10).